

Small Magellanic Cloud field stars meddling in star cluster age estimates

2 ANDRÉS E. PIATTI^{1,2}

3 ¹*Instituto Interdisciplinario de Ciencias Básicas (ICB), CONICET-UNCUYO, Padre J. Contreras 1300, M5502JMA, Mendoza,*
4 *Argentina*

5 ²*Consejo Nacional de Investigaciones Científicas y Técnicas (CONICET), Godoy Cruz 2290, C1425FQB, Buenos Aires, Argentina*

ABSTRACT

6 I revisited the age of the Small Magellanic Cloud cluster HW 42, whose previous estimates differ in
7 more than 6 Gyr, thus challenging the most updated knowledge of the SMC star formation history. I
8 performed an analysis of number stellar density profiles at different brightness levels; carried out a field
9 star decontamination of the cluster color-magnitude diagram; and estimated the cluster fundamental
10 parameters from the minimization of likelihood functions and their uncertainties from standard boot-
11 strap methods. I conclude that HW 42 is a $6.2^{+1.6}_{-1.3}$ Gyr old ($[\text{Fe}/\text{H}] = -0.89^{+0.10}_{-0.11}$ dex) SMC cluster
12 projected on to a SMC composite star field population which shows variations in magnitude, color,
13 and stellar density of Main Sequence stars. The present outcome solves the conundrum of the previous
14 age discrepancies and moves HW 42 to a region in the SMC age-metallicity relationship populated by
15 star clusters.

16 *Keywords:* techniques: photometric – galaxies: Magellanic Clouds – galaxies: star clusters: HW 42

1. INTRODUCTION

17 There is a general consensus that the oldest SMC star cluster population has ages ~ 6 -10 Gyr (Narloch et al. 2021,
18 and references therein). HW 42 is a SMC star cluster added to the group of intermediate-age star clusters by Piatti
19 (2011), and latter analyzed by Perren et al. (2017), who estimated an age of 5.0 Gyr from relatively shallow photometric
20 data. Recently, Bica et al. (2022) derived a much younger age (2.6 Gyr), moving it toward an extreme position in the
21 SMC star cluster age-metallicity relationship. The curious younger age and more metal-rich content ($[\text{Fe}/\text{H}]=-0.57$)
22 of HW 42 caught our attention.

2. DATA ANALYSIS AND DISCUSSION

23 In order to provide an independent estimate of the HW 42's age, I chose the publicly available Survey of the
24 Magellanic Stellar History (SMASH) DR2 data sets (Nidever et al. 2021). Since SMASH provides individual $E(B-V)$
25 values, I employed a dereddened g_0 versus $(g-i)_0$ CMD. After extensively examining the cluster CMD I found that
26 observed Main Sequence (MS) and Red Giant Branch (RGB) stars have distinguishable spatial distributions. I arrive
27 at this conclusion by building stellar number density profiles for stars at five different magnitude interval of 0.5 mag
28 wide from 20.0 down to 22.5 mag and located to the left or to the right of the lines drawn in Fig. 1.

29 A close inspection of Fig. 1 reveals that there is some excess of MS stars inside a radius of $\sim 0.5'$, only for stars with
30 $20.5 < g_0$ (mag) < 21.0 . For the remaining g_0 magnitude bins, number density dispersion around the mean background
31 level or lack of stars inside a radius of $\sim 0.5'$ prevail. If the excess of stars at $20.5 < g_0$ (mag) < 21.0 corresponds to the
32 cluster stellar population, and I assume that they are at the cluster MS turnoff, then HW 42 should be as young as 2.0
33 Gyr old. However, I would also expect to find fainter excesses of cluster MS stars, which is not the case. Additionally,
34 Fig. 1 shows excesses of RGB stars mostly along the whole magnitude range and inside a radius of $\sim 0.50'$, which
35 suggest the existence of an older stellar aggregate. Furthermore, it is not possible to reconcile a cluster MS turnoff as
36 bright as $g_0 \sim 20.5$ -21.0 mag with a lower end of a cluster RGB located at $g_0 \sim 22.5$ mag (Bressan et al. 2012). From
37
38
39

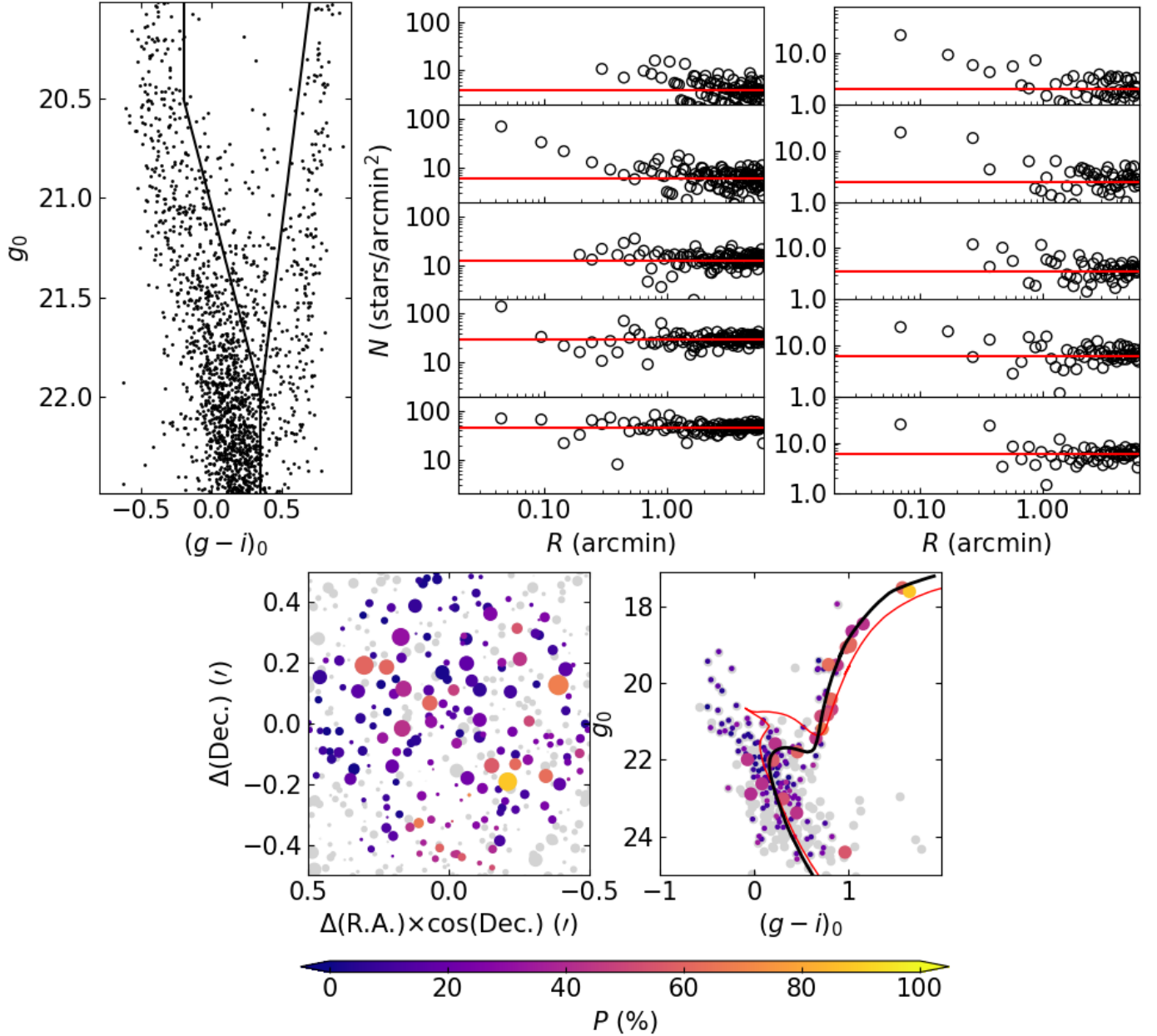


Figure 1. *Top:* CMD of stars located around a radius of $2'$ from the cluster center (left panel) and number density profiles for different magnitude bins and for MS (middle panel) and RGB (right panel) stars. Red lines represent the mean background level. *Bottom:* Chart of all stars measured in the field of HW 42 of its CMD. The size of the symbols in the chart is proportional to the g_0 brightness of the star. Symbols in both panels are color-coded according to the assigned membership probability P . Theoretical isochrones in [Bica et al. \(2022\)](#) and in this work are superimposed in the CMD with red and black lines, respectively.

40 Fig. 1 I conclude that I am dealing with the SMC MS field star contamination that misleads the reliable identification
 41 of the cluster MS turnoff. Indeed, I used to recognize star members of HW 42 the widely recommended HDBSCAN
 42 (Hierarchical Density-Based Spatial Clustering of Applications with Noise, [Campello et al. 2013](#)) Gaussian mixture
 43 model technique ([Hunt & Reffert 2021](#)), with SMASH coordinates as cluster searching variables, and the resulting
 44 most probable group includes MS field stars.

45 In order to confidently decontaminate the cluster CMD from field stars, I applied the procedure devised by [Piatti &](#)
 46 [Bica \(2012\)](#), which has been shown to produce cleaned cluster CMDs (e.g., [Piatti & Lucchini 2022](#); [Piatti 2022](#), and
 47 references therein). The cleaning procedure was applied a thousand times, each execution with a different randomly

selected reference field star region. From all the produced cleaned cluster CMDs, I defined the membership probability P (%) = $N/10$, where N represents the number of times a star was not subtracted during the thousand different CMD cleaning executions. Fig. 1 shows the spatial distribution and the CMD of stars with $P > 0\%$. As can be seen, a relatively long cluster RGB is clearly visible, alongside some few sub-giant and MS stars with $P > 50\%$.

I used theoretical isochrones computed by Bressan et al. (2012, PARSEC¹) for the SMASH photometric system to produce synthetic CMDs. PARSEC v1.2S isochrones spanned $\log(\text{age} / \text{yr})$ from 9.0 up to 9.9 in steps of 0.025, and metallicities ($\log(Z/Z_{\odot})$) from 0.0005 dex up to 0.005 dex, in steps of 0.001 dex. The Automated Stellar Cluster Analysis code (ASteCA, Perren et al. 2015) was employed to simultaneously derive the metallicity, the age, and the distance of HW 42, which resulted to be those corresponding to the isochrone associated to the synthetic CMD that best matched the cleaned dereddened cluster CMD ($P > 50\%$). The uncertainties in the derived parameters were estimated from the standard bootstrap method (Efron 1982). The resulting astrophysical properties of HW 42 turned out to be: distance = $54.45^{+2.83}_{-2.69}$ kpc (true distance modulus = 18.68 ± 0.11 mag); age = $6.2^{+1.6}_{-1.3}$ Gyr; and $[\text{Fe}/\text{H}] = -0.89^{+0.10}_{-0.11}$ dex.

The cleaned cluster CMD shows a numerous population of MS stars - there are also some sub-giant and giant stars - with $P < 10\%$. These stars belong to the SMC field star population, and remain in the cleaned cluster CMD because of their not homogeneous distribution in either magnitude, color, stellar density or all of these three quantities combined across the cluster field of view. As can be seen, HW 42 (stars with distance to the cluster center $< 0.5'$) is projected on to a composite field population with MS stars spanning an age range of ~ 1 -6 Gyr. Such an SMC MS field star contamination is also seen in the cluster CMD built by Bica et al. (2022). Fig. 1 shows that the cluster MS turnoff arising from this work is fainter than that adopted by Bica et al. (2022)

This research uses services or data provided by the Astro Data Lab at NSF's National Optical-Infrared Astronomy Research Laboratory. NSF's OIR Lab is operated by the Association of Universities for Research in Astronomy (AURA), Inc. under a cooperative agreement with the National Science Foundation.

REFERENCES

- Bica, E., Maia, F. F. S., Oliveira, R. A. P., et al. 2022, MNRAS, 517, L41, doi: [10.1093/mnras/slac108](https://doi.org/10.1093/mnras/slac108)
- Bressan, A., Marigo, P., Girardi, L., et al. 2012, MNRAS, 427, 127, doi: [10.1111/j.1365-2966.2012.21948.x](https://doi.org/10.1111/j.1365-2966.2012.21948.x)
- Campello, R. J. G. B., Moulavi, D., & Sander, J. 2013, In: Pei, J., Tseng, V.S., Cao, L., Motoda, H., Xu, G. (eds) Advances in Knowledge Discovery and Data Mining. Lecture Notes in Computer Science(), vol 7819. Springer, Berlin, Heidelberg.
- Efron, B. 1982, The Jackknife, the Bootstrap and other resampling plans
- Hunt, E. L., & Reffert, S. 2021, A&A, 646, A104, doi: [10.1051/0004-6361/202039341](https://doi.org/10.1051/0004-6361/202039341)
- Narloch, W., Pietrzyński, G., Gieren, W., et al. 2021, A&A, 647, A135, doi: [10.1051/0004-6361/202039623](https://doi.org/10.1051/0004-6361/202039623)
- Nidever, D. L., Olsen, K., Choi, Y., et al. 2021, AJ, 161, 74, doi: [10.3847/1538-3881/abceb7](https://doi.org/10.3847/1538-3881/abceb7)
- Perren, G. I., Piatti, A. E., & Vázquez, R. A. 2017, A&A, 602, A89, doi: [10.1051/0004-6361/201629520](https://doi.org/10.1051/0004-6361/201629520)
- Perren, G. I., Vázquez, R. A., & Piatti, A. E. 2015, A&A, 576, A6, doi: [10.1051/0004-6361/201424946](https://doi.org/10.1051/0004-6361/201424946)
- Piatti, A. E. 2011, MNRAS, 416, L89, doi: [10.1111/j.1745-3933.2011.01105.x](https://doi.org/10.1111/j.1745-3933.2011.01105.x)
- . 2022, MNRAS, 514, 4982, doi: [10.1093/mnras/stac1274](https://doi.org/10.1093/mnras/stac1274)
- Piatti, A. E., & Bica, E. 2012, MNRAS, 425, 3085, doi: [10.1111/j.1365-2966.2012.21694.x](https://doi.org/10.1111/j.1365-2966.2012.21694.x)
- Piatti, A. E., & Lucchini, S. 2022, MNRAS, 515, 4005, doi: [10.1093/mnras/stac1980](https://doi.org/10.1093/mnras/stac1980)

¹ <http://stev.oapd.inaf.it/cgi-bin/cmd>